HF Resonators for Damping of VFTs in GIS

J. Smajic, W. Holaus, A. Troeger, S. Burow, R. Brandl, S. Tenbohlen

Abstract—**A novel technique for damping of very fast transient overvoltages in gas insulated switchgears based on high frequency resonators is presented. Two different numerical algorithms based on full-Maxwell time-domain and frequency-domain electromagnetic field simulations for the design of HF resonators are described. The predictive power of the algorithms is validated by experiment. The damping effect of the suggested solution is confirmed by measurements.**

Keywords: **Very fast transients, Gas insulated switchgear, and high frequency resonator.**

I. INTRODUCTION

VERY fast transients (VFTs) in high voltage gas insulated switchgears (GIS) are electromagnetic waves initiated by the GIS disconnector switching operations [1]. Propagating along a GIS and being multiply reflected from the GIS terminations, VFTs have a non-harmonic time dependence and cover a wide frequency range from 100kHz-100MHz [1], [2].

As already reported in [2], they are presently a limiting constraint for the dielectric design of ultra high voltage (UHV) GIS with a rated voltage of 1100kV (AC). Therefore, the modeling and simulations of VFTs are of paramount importance for estimating their peak values and designing efficient damping components [2].

The damping of VFTs in UHV GIS by using a resistor fitted disconnector was reported in [3]. The achieved damping efficiency was rather high, but this solution is very costly and makes the dielectric and mechanical design of the disconnector much more demanding. As an alternative, the VFT damping solution utilizing ferrite rings have been also analyzed and tested [4]. The measurements show that the damping effect can be achieved, but with an important drawback: the magnetic material goes easily into saturation, which complicates the design and reduces its generality and robustness.

The aim of this paper is manifold: (a) to present a novel approach for damping of VFTs by using compact electromagnetic high-frequency (HF) resonators with low quality (Q) factor specially designed to cover a wider frequency range; (b) to describe two different simulation algorithms for the full-Maxwell eigenvalue analysis of the resonator; and (c) to demonstrate the resonator's damping efficiency.

The novelty of this idea is not only in designing the low Q resonators but also in dissipating the received VFT energy by igniting an electric arc in the electrically shielded SF6 gap of the resonator [5].

The rest of the paper is organized as follows: Section II describes the time-domain and frequency-domain full-Maxwell eigenvalue analysis of the resonator. Section III contains the numerical results and their experimental verification. Section IV concludes the paper.

II. EIGENVALUE ANALYSIS OF HF RESONATORS

HF resonators for damping of VFTs in GIS should have a special geometrical shape not to hinder the GIS dielectric design. From the dielectric design viewpoint, a suitable shape of the resonator should be elongated along the GIS conductor axis in order to achieve a low enough resonant frequency with a minimum size in the radial direction. In addition to this the outer surface of the resonator should be smooth (rounded) in order to avoid electric field enhancement regions such as sharp edges and corners.

A promising resonator geometry that fulfils the described constraints is shown in Figure 1. In the radial direction the resonator is not significantly larger than the GIS conductor, leaving enough clearance distance to the enclosure. To increase the cavity volume and reduce the resonance frequency the radius of the GIS conductor inside the resonator is reduced. Since the magnetic field of the resonator is distributed over the cavity volume, the cavity size will determine the resonator magnetic inductance (L). As visible in Figure 1, on the left hand side of the resonator a gap of some millimeters between the resonator and inner GIS conductor is made. This is the space of an electric field enhancement, i.e. the space that determines the resonator electric capacitance (C).
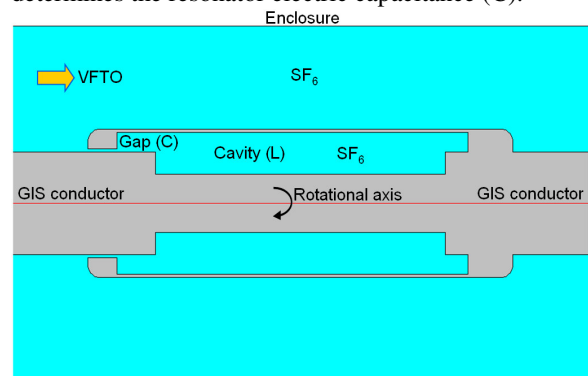

Fig. 1. The axisymmetric geometry of the HF resonator.

J. Smajic is with ABB Switzerland Ltd. Corporate Research, Segelhofstrasse 1K, CH-5405 Baden-Dättwil, Switzerland,
(e-mail: jasmin.smajic@ch.abb.com).

W. Holaus and A. Troeger are with ABB Switzerland Ltd., Brown-Boveri-Strasse 5, CH-8050 Zurich, Switzerland,
(e-mail: walter.holaus@ch.abb.com).

S. Burow, R. Brandl, and S. Tenbohlen are with Universität Stuttgart Pfaffenwaldring 47, D-70569 Stuttgart, Germany,
(e-mail: simon.burow@ieh.uni-stuttgart.de).

Having the resonator inductance and capacitance it is possible to compute its resonance frequency $f = 1/\left(2\pi\sqrt{LC}\right)$. However, for the resonator geometry presented in Figure 1 or for any other geometry in general, it is not possible to analytically compute its L and C.

A general solution of this problem is the so-called eigenvalue analysis (resonance search) of a resonator based on full-Maxwell electromagnetic field simulations [6] that is presently a common approach for the design of microwave resonators. In this approach the source-free Maxwell equations are discretized by using the finite element method (FEM). This process results in a large sparse homogenous system of linear equations. The mathematical eigenvalues of this system correspond to the resonance frequencies of the resonator [6, 7]. Although general and mathematically elegant, this method of microwave engineering is not suitable for our analysis of HF resonators. There are two main reasons for this: (a) our resonator is an open boundary problem, and (b) it is strongly coupled with the incoming and outgoing GIS conductors.

A. Time-Domain Eigenvalue Analysis

Our first numerical method that is very suitable for the eigenvalue analysis of open HF resonators is based on the time-domain solution of the following boundary-initial value problem:

$$\nabla \times \left(\frac{1}{\mu_r}\nabla \times \vec{A}\right) + \mu_0\sigma\frac{\partial \vec{A}}{\partial t} + \mu_0\varepsilon_0\frac{\partial}{\partial t}\left(\varepsilon_r\frac{\partial \vec{A}}{\partial t}\right) = 0 \qquad (1)$$

$$\vec{n} \times \vec{A} = 0 \text{ (PEC BC)} \qquad (2)$$

$$Z_{port} = \frac{U_{port}}{I_{port}} \text{ (Lumped port with voltage input)} \qquad (3)$$

$$\vec{A}(\vec{r},0) = 0 \text{ (Zero initial condition)} \qquad (4)$$

Where $\vec{A}$ is the magnetic vector potential, PEC BC stands for the perfect electric conductor boundary condition, $\vec{n}$ is the normal unit vector to the PEC boundary, μ_0 is the magnetic permeability of vacuum, μ_r is the relative magnetic permeability, ε_0 is the electric permittivity of vacuum, ε_r is the relative electric permittivity, and Z_{port} is the wave impedance of a lumped port.

The termination of the structure and its connection with the voltage source described by (3) has, in our simulations, the following field representation [2, 6]:

$$-\vec{n} \times \left(\frac{1}{\mu_r}\nabla \times \vec{A}\right) - \frac{\mu_0}{Z_{PORT}}\frac{\partial}{\partial t}\vec{n} \times \left(\vec{n} \times \vec{A}\right) = \frac{2\mu_0}{Z_{PORT}}\vec{n} \times \left(\vec{n} \times \vec{E}_0\right) \qquad (5)$$

As reported in [2] this method is general and was successfully applied to 3D simulations of VFTs in GIS. In addition to this, which is one of the main points of this paper, this method can be modified and applied to eigenvalue analysis of HF resonators.

Once the boundary-initial value problem (1-5) is solved, the A-field solution over the entire computational domain for a given interval of time is obtained. The magnetic flux density (B) and magnetic field (H) can be computed from the A-field solution by using the following equations [8]:

$$\vec{B} = \nabla \times \vec{A}, \quad \vec{H} = \frac{\vec{B}}{\mu_0\mu_r} = \frac{\nabla \times \vec{A}}{\mu_0\mu_r} \qquad (6)$$

The electric field (E) can be obtained from the third Maxwell equation [8]:

$$\nabla \times \vec{E} = -\frac{\partial \vec{B}}{\partial t} \stackrel{(6)}{\Rightarrow} \vec{E} = -\frac{\partial \vec{A}}{\partial t} \qquad (7)$$

The electric voltage (U) between two different points (P_1 and P_2) of the simulation model could be obtained by integrating the electric field along a given path between these two points [8]:

$$U = \int_{P_1}^{P_2} \vec{E} \cdot d\vec{l} = -\int_{P_1}^{P_2} \frac{\partial \vec{A}}{\partial t} \cdot d\vec{l} \qquad (8)$$

Since dynamic electromagnetic fields are under consideration the voltage definition (8) is not unique but dependent on the chosen path between P_1 and P_2. Hence, the voltage calculated by (8) is in general not a useful quantity. However, in some practically important cases the voltage (8) is uniquely defined. In order for the voltage definition (8) to be unique it is necessary that the following holds [8]:

$$\oint_{(C)} \vec{E} \cdot d\vec{l} = -\oint_{(C)} \frac{\partial \vec{A}}{\partial t} \cdot d\vec{l} = 0 \qquad (9)$$

Evidently, this is in general not fulfilled because of the following equation [8]:

$$\oint_{(C)} \vec{E} \cdot d\vec{l} \stackrel{(Stockes')}{=} \iint_{(A)} \nabla \times \vec{E} \cdot d\vec{l} \stackrel{(Maxwell)}{=} -\iint_{(A)} \frac{\partial \vec{B}}{\partial t} \cdot d\vec{l} \neq 0 \qquad (10)$$

It is important to notice that the condition (9) or zero-condition (10) holds in some practical cases, namely the cases in which the contour (C) or its area (A) are tangential to the magnetic field lines. In this case the voltage definition (8) is unique over the entire plane and could be used for some numerical comparisons and valid conclusions.

For example, the geometry presented in Figure 1 is exactly this case. If the VF current flows along the resonator and attached GIS conductors, the corresponding magnetic field will have only the phi-component in the adjacent cylindrical coordinate system. This means that over each plane, perpendicular to the resonator axis, the condition (9) holds and the voltage (8) is uniquely defined and could be used for obtaining relevant conclusions.

Let us consider the simulation model presented in Figure 2. The resonator introduced in Figure 1 is connected to two GIS cylindrical conductors. The left hand side conductor is terminated by a voltage source of certain impedance and the right hand side conductor is assumed to be infinitely long. The impedance of the generator Z_g is assumed to be equal to the wave impedance of the cylindrical GIS conductor- enclosure
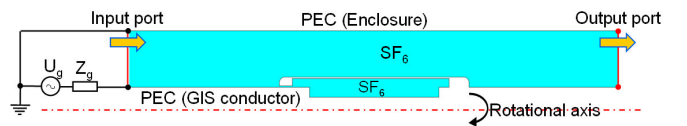

Fig. 2. The axisymmetric 2D simulation model suitable for eigenvalue analysis of the HF resonator from Figure 1 based on full-Maxwell time-domain FEM.

combination so that no wave reflections occur at the input port. The input port is then accurately described by Equations (3) and (5).

Considering the VFT frequency range (100kHz-100MHz) it is realistic to assume all the metallic parts of the resonator, GIS conductor and enclosure as perfect conductors (PEC).

The output port of the simulation model can also be described by Equation (5) with zero right hand side (source free). Thus, if the port impedance Z_{PORT} is adjusted to the wave impedance of the cylindrical GIS conductor-enclosure combination, no fictitious wave reflections occur at the output port.

To perform an eigenvalue analysis of the resonator in time-domain, the voltage source U_g should generate a very special impulse presented in Figure 3 (left). This is the so-called Gaussian burst, a well-known mathematical function that could be defined in time-domain so that it covers a desired spectrum in frequency-domain:

$$y_1(t) = C_1 \cdot e^{-\alpha(t-t_0)^2} \tag{11}$$

$$y_2(t) = C_2 \cdot sin(2\pi f_0 \cdot t) \tag{12}$$

$$y_{Gaussian\,burst}(t) = y_1(t) \cdot y_2(t) \tag{13}$$

Gaussian burst is an amplitude modulation of the harmonic function (12). The modulation function (11) is a Gaussian exponential function with the peak at the t_0 moment of time. The impulse width τ (Figure 3 – left) is determined by the parameter α in Equation (11). According to [9], the Fourier transformation of the burst (13) is also a Gaussian exponential function in frequency domain (Figure 3 – right) with the width Φ around the central frequency f_0. Thus, by defining Gaussian burst in time-domain by Equations (11-13), it is possible to control the corresponding frequency range of interest in frequency-domain as illustrated in Figure 3.

If the voltage source generates the burst presented in Figure 3, the corresponding electromagnetic waves will travel along the GIS conductors and over the resonator, eventually leaving the system through the output port. The time-domain electromagnetic field simulation based on FEM discretization of the boundary-initial value problem (1-5) reveals the electromagnetic field in the computation domain.

The electric field integration across the gap of the resonator over time yields the gap voltage that has, in this simulation setup, rather complicated time-dependence. However, the discrete Fourier transform of the gap voltage should show the response of the resonator in frequency-domain, i.e. it should reveal the resonant frequencies. Essentially, this is the main idea behind our time-domain eigenvalue analysis.

B. Frequency-Domain Eigenvalue Analysis

By applying Fourier transforms to the boundary-initial value problem (1-5), the equivalent boundary value problem in frequency-domain is obtained. For a given frequency and voltage of the source U_g (that is now a harmonic source) this
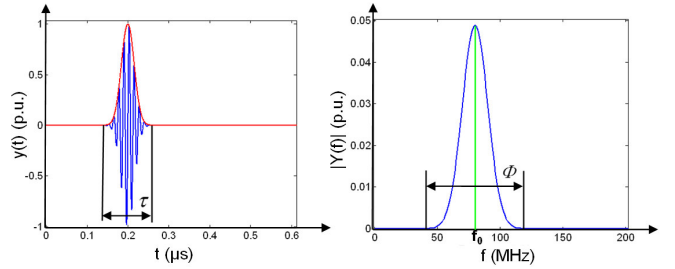

Fig. 3. The well-known Gaussian burst in time-domain (left) and its Fourier transformation in frequency-domain.

problem could be also solved and the corresponding electromagnetic field in the computational domain, as well as the resonator's gap voltage could be obtained. By changing the source frequency over a desired frequency range, the functional dependence of the gap voltage and frequency could be revealed. Sharp tips of this curve correspond to the required resonant frequencies. This essentially describes the main idea behind our frequency-domain eigenvalue analysis.

Since these two simulation algorithms have very different theoretical background and require different simulation models, they are very useful for result verification by comparison against each other.

Considering experimental determination of the resonant frequencies, the second frequency-domain approach seems to be more suitable. Therefore this frequency-domain approach has been used for the resonance measurements presented in the paper.

III. NUMERICAL RESULTS

The described time-domain and frequency-domain eigenvalue analysis of the resonator presented in Figure 1 were performed. In order to experimentally verify the obtained results the resonator was also manufactured and tested by using the frequency-domain approach similar to the simulation setup presented in Figure 2.

For the measurement the resonator was mounted on a short part of GIS with cones on each side. A third orifice of the GIS enables a direct access to the resonator. Figure 4 shows the resonator testing setup which was used for the measurements. On the left end side a waveform generator was connected via a BNC plug to the test setup. On the right end side a terminating impedance was placed so that reflection was avoided. The output of the waveform generator was a sinusoidal signal with an amplitude of 10 V. By steps of 1 MHz the frequency of the signal was shifted from 1 MHz up to 100 MHz. The voltage in the gap between resonator and GIS conductor was measured by a special kind of field probe made by university of Stuttgart.
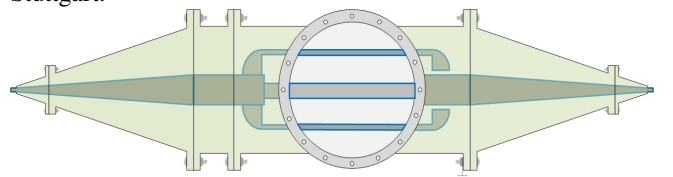

Fig. 4. The resonator testing setup: GIS with cones on each side and the resonator mounted on the inner conductor.

The numerical results obtained by using the two described methods were compared against each other and against measurements. This comparison is shown in Figure 5.

Evidently, both simulation results agree very well with the measurements. It is important to mention that the goal of the simulations and measurements was to reveal the resonant frequency of the resonator and not to determine the value of the resonator's gap voltage. The value of the voltage highly depends on the source characteristics as well as on the measurement setup.
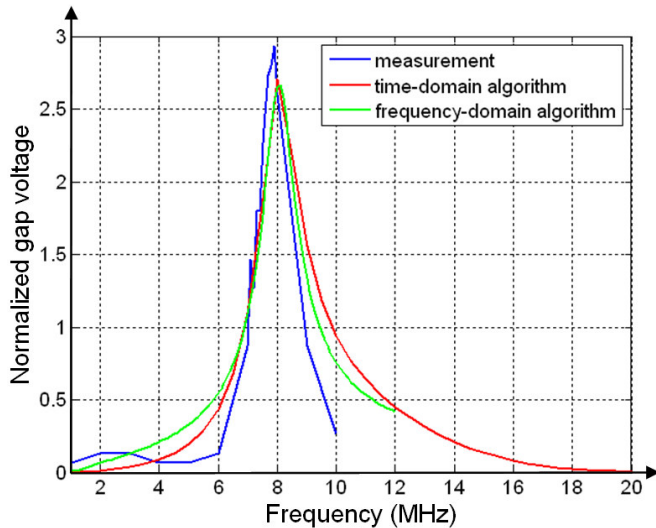

Fig. 5. Eigenvalue analysis results of the HF resonator for VFT damping from Figure 1 and Figure 4.

It is also interesting to visualize the electric and magnetic field of the resonator at the resonance. These fields are shown in Figure 6. As anticipated the electric field is confined to the resonator's gap in order to ignite an electric spark and to dissipate the VFT energy, and the magnetic field is distributed over the resonator's cavity.

The fields in Figure 6 justify the representation in Figure 1 showing that the equivalent capacitance of the resonator is
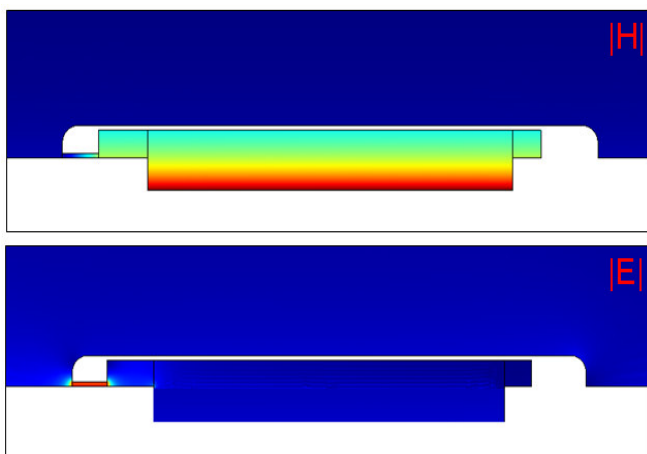

Fig. 6. The electric (bottom) and magnetic field of the HF resonator at resonance frequency (8MHz).

determined by the gap and the inductance by the volume of the resonator's cavity. This is very important information for tuning the resonator to the desired resonant frequency.

The presented electromagnetic field simulations have been done by using the commercial time- and frequency-domain FEM solver COMSOL [10].

To check its VFT damping effect, the resonator was mounted on the testing installation of the ABB GIS type ELK-3 at the University of Stuttgart. The VFTs in the GIS are generated by a standard HV impulse generator. Via a bushing the surge voltage reaches an electric spark gap inside the GIS with spherical contacts. The other side of the spark gap is grounded. If the breakdown voltage of the spark gap is reached, a sparkover occurs in the SF_6 – atmosphere and causes the VFTs. The VFT testing equipment is presented in Figure 7.

Fig. 7. The ABB 550kV GIS type ELK-3 for testing purposes at the University of Stuttgart.
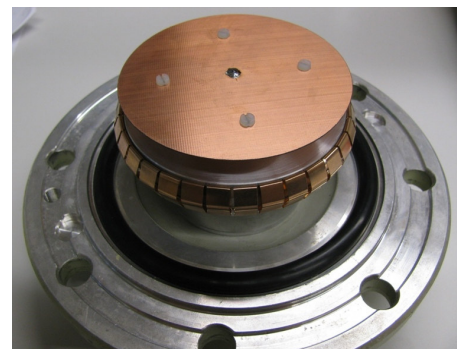

Fig. 8. The sensors which are made at the University of Stuttgart. They consist mainly of a double layer board and form a capacitive voltage divider.

Two special manufactured capacitive sensors are mounted inside the GIS and enable a very precise measurement of the VFT-voltage. The sensors consist mainly of a double layer board and are presented in Figure 8. One layer is connected to the grounded GIS enclosure. The second layer forms a capacity as well to the grounded layer as to the inner conductor of the GIS. So a capacitive voltage divider is arranged and the voltage of VFTs could be measured.

The signals of the Sensors are recorded by an Oscilloscope (LeCroy waveRunner 104 MXi, used Bandwidth: 200 MHz). Before analyzing the results, always 10 signals are superimposed to avoid impacts caused by small variation of the breakdown voltage. The frequency spectrum of the results is computed by a Fast Fourier Transform with Matlab.
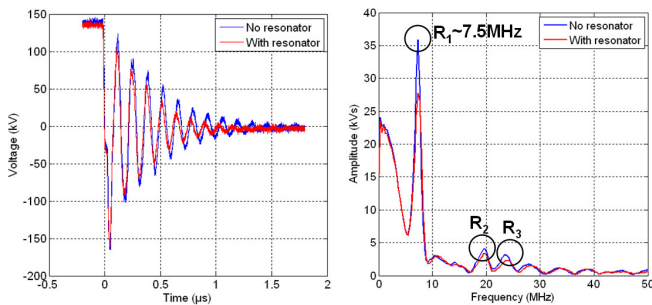

Fig. 9. The VFTs in time (left) and frequency domain of the ABB 550kV GIS type ELK-3 with and without the resonator are shown. Evidently, the dominant 7.5MHz harmonic component (R_1) of the VFTs was significantly reduced. For the reason of simplicity the onset and propagation of the VFTs is measured at the voltage level much lower than the rated voltage.

The initial results of this test are presented in Figure 9. Evidently, the dominant harmonic component (R_1) of the VFT was significantly reduced (25%). Since the parameters of the resonator could be changed in a wide range, the resonator could be optimized in the future in order to increase its damping efficiency.

IV. CONCLUSIONS

The time-domain and frequency-domain method for eigenvalue analysis of HF resonators for damping of VFTs in GIS was presented. The predictive power of the methods was verified by comparison against each other and against measurements. The suggested methods are simple enough to be used in the GIS design process.

The VFT damping effect of the developed HF resonator tuned to the dominant harmonic component of VFTs of the real-life GIS was confirmed by experiments.

VI. REFERENCES

[1] J. Meppelnik, K. Diederich, K. Feser, W. Pfaff, "Very Fast Transients in GIS", *IEEE Transactions on Power Delivery*, Vol. 4, No. 1., pp. 223 - 233, 1989.
[2] J. Smajic, W. Holaus, J. Kostovic, U. Riechert," 3D Full-Maxwell Simulations of Very Fast Transients in GIS", Accepted for publication in *IEEE Transactions on Magnetics*, 2010.
[3] Y. Yamagata, K. Tanaka, S. Nishiwaki, "Suppression of VF in 1100kV GIS by Adopting Resistor-fitted Disconnector", *IEEE Transactions on Power Delivery*, Vol. 11, No. 2, pp. 872 – 880, 1996.
[4] W. D. Liu, L. J. Jin, J. L. Qian, "Simulation Test of Suppressing VFT in GIS by Ferrite Rings", in *Proceedings of 2001 International Symposium on Electrical Insulating Materials*, pp. 245-247, 2001.
[5] W. Holaus, J. Smajic, J. Kostovic, "High-Voltage Device and Method for Equipping a High-Voltage Device with Means for Reducing Very Fast Transients (VFTs)", Patent No. 09156418.7-1242, European Patent Office, March 27, 2009.
[6] J. Jin, *The Finite Element Method in Electromagnetics*, 2nd Edition, Wiley-IEEE Press, New York, 2002.
[7] G.H.Golub and Ch.F .Van Loan, *Matrix Computations*, 3rd edn., Johns Hopkins University Press, Baltimore, 1996.
[8] J. D. Jackson, "Classical Electrodynamics", Third Edition, John Wiley & Sons Inc., New York, 1999.
[9] S. W. Smith, "Digital Signal Processing : A Practical Guide for Engineers and Scientist", Elsevier Science, New York, 2003.
[10] COMSOL Multiphysics, www.comsol.com.